Investigations on the temperature-deformation behaviour of advanced high-strength steel sheets (AHSS) under shear loading from nearly isothermal to the adiabatic state

S. Klitschke[1*], M. Liewald[2]

[1] Fraunhofer Institute for Mechanics of Materials IWM, Freiburg, Germany
[2] Institute for Metal Forming Technology, University of Stuttgart, Germany
*Corresponding author. Email: silke.klitschke@iwm.fraunhofer.de

Abstract

Steel sheet materials tend to form adiabatic shear bands at high strain rates, leading to material separation. This phenomenon is used in adiabatic blanking processes, but it should be avoided in crash safety applications. This paper deals with investigations on the main influence parameters on adiabatic heating of advanced high strength steel sheets (AHSS) under shear loading. Focussing on the effect of applied strain rate, experimental investigations were carried out from quasi-static loading up to crash-relevant strain rates. Strain and temperature fields were recorded using a high-speed video camera and a high-speed infrared camera, thus enabling a detailed analysis of the generated heat and the heat transport mechanisms in the deformed zones. The examination showed that the isothermal-adiabatic transition under shear loading ranges between strain rates of 0,01 s^{-1} up to 50 s^{-1} for the investigated materials and thus at higher strain rates compared to tensile loading. This indicates an extreme strain localization in shear bands compared to necking zones at comparable strain rates. Consequently, larger temperature gradients occur in the shear zone, which significantly affect the heat transfer mechanisms. Furthermore, with increasing strain hardening, the isothermal-adiabatic transition region is also shifted to higher strain rates due to a slowdown of the strain and temperature localization process. Based on these results, local heating and the occurrence of adiabatic shear bands can be estimated without costly thermomechanical coupling finite element simulations (FE-Simulations).

Keywords

High strength steel, Metal forming, Thermal effect

1 Introduction

In highspeed forming processes and in crash scenarios highly dynamic loads occur and cause local temperature increases of several hundred Kelvin, particularly in advanced high strength steel sheets (AHSS). Under large strain rates steel materials in general show a tendency to develop adiabatic shear bands leading to material segregation, as initially demonstrated by Kravz-Tarnavskii (1928). This phenomenon is used in adiabatic blanking processes. Due to significant lower shear failure strains under high strain rates compared to quasi-static shear loading, observed e.g. by Peiers and Verleysen (2012), it is imperative to prevent it in crash safety applications. In both scenarios, it is critical to determine the range of strain rates at which adiabatic shear bands (ASB) occur, in order to induce or prevent shear failure. Additionally, estimating heat dissipation is essential for optimizing computational efficiency without resorting to thermomechanically coupled simulations.

Shear bands develop under complex thermokinetic conditions. The main results in literature are summarized by Walley (2007) and Dodd (2015). Under nearly adiabatic conditions temperature rise depends on the amount of locally dissipated plastic deformation energy converted into heat. Taylor and Quinney (1934) and Davidenkov and Mirolubov (1935) found that for metals plastic work is not completely transformed into heat. The percentage of plastic work converted into heat, characterized by the Taylor-Quinney coefficient (TQC), is assumed to be nearly constant as 90% for steels, according to Rittel (2017) under uniaxial and shear loading. The heat transfer in metals, primarily governed by thermal conduction, depends not only on thermal conductivity but particularly on the temperature gradient.

The objective of this study was to explore the factors impacting the isothermal-adiabatic transition region, especially in the presence of shear bands. Consequently, the primary influencing parameters affecting adiabatic heating in AHSS were experimentally examined, with a specific emphasis on shear loading vs. tensile loading. A comprehensive investigation into the heat generated and the heat transfer mechanisms within the intensely deformed regions was conducted through tensile and shear tests across a local strain rate spectrum ranging from approximately 0.001 s^{-1} to 50 s^{-1}.

2 Experimental investigations

2.1 Materials and test setup

The main investigations of the present study were carried out on a micro-alloyed steel HX340LAD and a dual-phase steel HCT980X. Further selective examinations were conducted on an additional dual-phase steel HCT980X+Z110MB and a complex-phase steel HCT780C, see **Table 1**. Uniaxial tensile tests and shear tensile tests were performed at test speeds between 0.02 and 25 mm/s, resulting in nominal strain rates from 0.001 s^{-1} to 1 s^{-1}. In the localized zones they induce larger strain rates, as discussed in chapter 2.3. Uniaxial tension tests utilized a flat tensile specimen geometry recommended in ISO 26203-2 (2011), which is well-suited for high strain rates. The shear tensile tests were conducted using an asymmetric shear notch tensile specimen, both geometries see **Fig. 1** left.

material	Sheet thickness in mm	$R_{p0.2}/R_{eL}$ in MPa	R_m in MPa	A_g in %	A_{20mm} in %	$n_{2\text{-}Ag}$	Z in %
HCT980XG	1.4	759	1049	7.1	13.4	0.08	33.5
HX340LAD	1.5	390	461	17.4	35.6	0.148	62.5
HCT780C	1.5	689	878	8.4	17.4	0.094	50.5
HCT980X+Z110MB	1.5	683	1007	10.3	18.5	0.132	35.1

Table 1: *Mechanical values 90° to rolling direction*

The tests were performed on a high-speed testing machine (Zwick 500/10). The local strain fields on the specimen surface were determined using a high-speed video camera of the Photron SA series and evaluation with 2D digital image correlation (DIC) using the GOM Correlate 2020 software. The temperature measurements were carried out on the back of the sample using a high-speed infrared dual-band camera (IR-camera) from the IRCAM GEMINIS 327k ML series. The force was measured using a piezo load cell. Based on the strain and temperature field measurements, the strain and temperature developments in the localized zones were evaluated. The von Mises equivalent strain was selected as the relevant strain variable, to be able to compare the temperature increase as a function of the local strain between the flat tensile and shear tensile tests, see **Fig. 1** right.

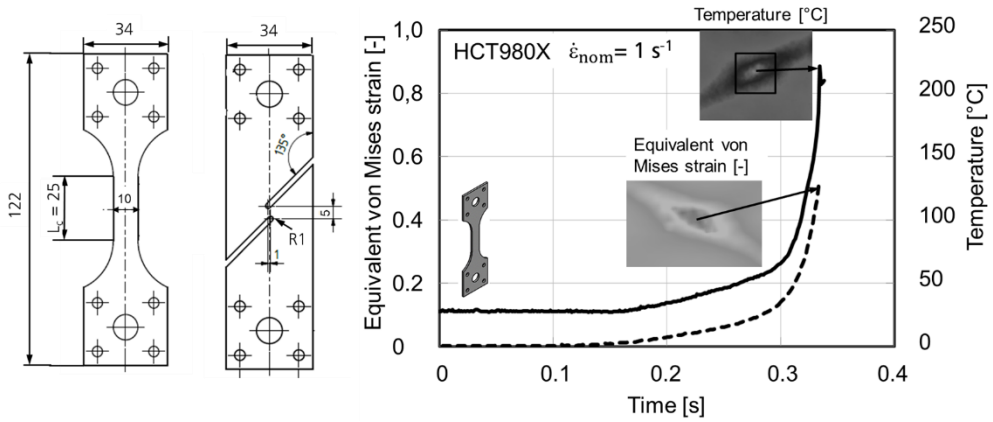

Figure 1*: Flat tensile and shear tensile geometry (left) and measured maximal local temperature and strain (right) for the dual-phase steel HCT980X*

2.2 Measured results

In all experiments, the local temperature rise was plotted against the local strain, as illustrated by the example of flat tensile tests on the micro-alloyed steel at various strain rates in **Fig. 2** on the left. Elevated strain rates corresponded to higher temperature increases. Nevertheless, for the comparative assessment of adiabatic temperature rise across distinct sheet materials, understanding the fraction of deformation energy retained in the form of heat is essential. This proportion is characterized by the ratio q/w of volume-specific thermal energy q to volume-specific plastic deformation work w within the localized region. The ratio q/w, defined as the "heat ratio", represents the fraction of plastic deformation work initially

transformed into heat quantified by the TQC, less the portion of energy dissipated through heat transfer.

w was determined according to equation (1) by the maximum local equivalent strain $\varepsilon_{v,max}$ in the necking area and the corresponding true equivalent stress $\sigma_{wahr,v}$. For uniaxial tensile tests $\sigma_{wahr,v}$ is calculated from the engineering stress assuming volume constancy and a homogeneous stress state over the thickness. Lateral forces in the clamping can be neglected due to the rotationally free mounting. For shear tests $\sigma_{wahr,v}$ is corrected because of the multiaxial stress state, assuming associated flow rule according to Andrade (2019).

q was calculated according to equation (2) by the measured temperature increase ΔT, a constant heat capacity c_p of 0.47 J/gK and a constant density ρ of 7.86 g/cm^3. According to Richter (2010) the heat capacity of microalloyed steels can vary by 10-15% between 20°C and 200°C, hence q might be moderately underestimated for larger temperatures.

$$w = \int_0^w dw = \int_0^{\varepsilon_{v,max}} \sigma_{wahr,v}\, d\varepsilon_{v,max} \quad (1)$$

$$q = \rho\, c_p\, \Delta T \quad (2)$$

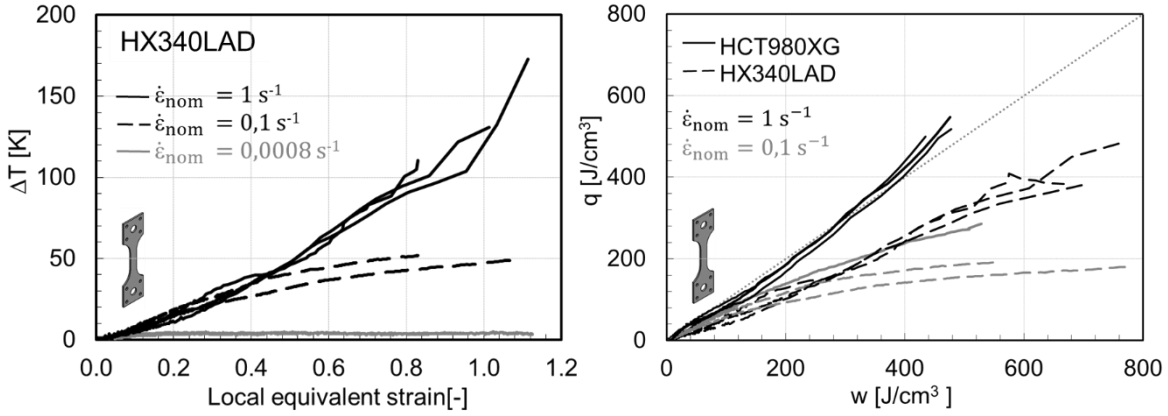

***Figure 2**: Measured local temperature increase dependent on the local equivalent strain at different strain rates for HX340LAD (left) and calculated local heat dependent on local plastic work at different strain rates for two materials (right) both for uniaxial tensile tests*

2.3 Evaluation of isothermal-adiabatic transition region

Not only the heat ratio q/w but also the local strain rate changes over the duration of the test, see **Fig. 3**. In order to obtain a correlation between heat ratio and equivalent strain rate for each test, the mean value of the heat ratio $\frac{\overline{q}}{w}$ and the mean value of the equivalent strain rate $\overline{\dot{\varepsilon}_v}$ was calculated between a material-dependent local initial strain, located around the start of necking, and the elongation at fracture, see **Fig. 3**.

The strain rate dependent heat ratio $\frac{\overline{q}}{w}(\bar{\varepsilon}_v)$ differs significantly for the different steel sheet materials, see **Fig. 4** on the left. For the micro-alloyed steel HX340LAD, the values for $\frac{\overline{q}}{w}(\bar{\varepsilon}_v)$ are lower than for the dual-phase steel HCT980XG at a comparable strain rate. Assuming a nearly constant TQC of about 90%, the micro-alloyed steel therefore exhibits more heat transfer at a comparable strain rate compared to the dual-phase steel. The transition range from isothermal to adiabatic can be determined between 0.01 s^{-1} and approximately 10 s^{-1} for the dual-phase steel and up to higher strain rates for the micro-alloyed steel. This difference could be due to different temperature gradients in the localized zone, which in turn could result from different strain gradients based on localizations pendent on material properties.

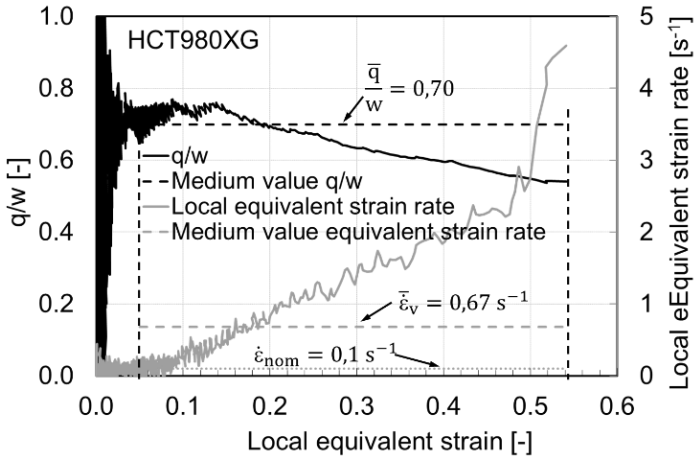

***Figure 3**: Mean value calculation for q/w and the equivalent strain rate in the range between 5% equivalent strain and failure strain using the example of a flat tensile test at a nominal strain rate of 0.1 s^{-1} for the sheet material HCT980XG*

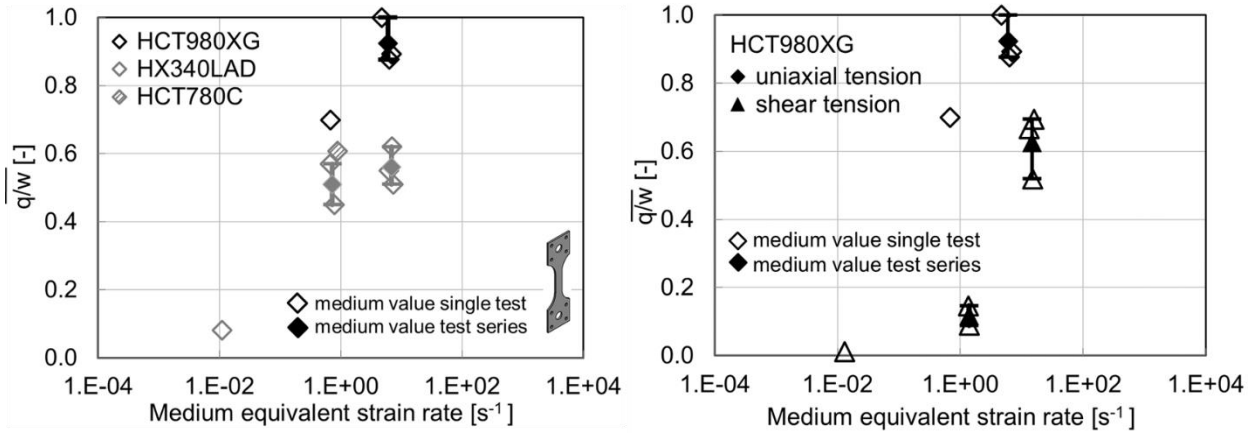

***Figure 4**: Average heat ratio as a function of the medium equivalent strain rate for various AHSS under tensile load (left) and for tensile and shear load for HCT980XG (right)*

For the shear tensile tests, the transition range between isothermal and adiabatic is found at higher strain rates compared to the flat tensile tests, see **Fig. 4** on the right. For a

strain rate of about 10 s^{-1} for example, the flat tensile tests show a heat ratio value $\frac{\overline{q}}{w}$(10 s^{-1}) of about 0.9 and therefore almost adiabatic conditions, while the shear tensile tests with a heat ratio value $\frac{\overline{q}}{w}$(10 s^{-1}) of about 0.6 are found still in the transition region between isothermal and adiabatic. It can therefore be assumed that under shear loading, more heat dissipation occurs from the shear bands into the surrounding material than it is the case with the necking zones under tensile loading at comparable strain rates.

2.4 Evaluation of strain localization

The temperature gradients that occur in the localized zone are due to the localized strains and are also mutually influenced by the local strain rates, the stress state (necking or shear band) as well as by material properties like the hardening value n and the heat conductivity λ. Due to these complex relationships, extended analyses were carried out on the influence of the material properties on the localization of the strains. Therefore a key value "strain localization" is defined according to equation (3) as the height of the strain peak $\varepsilon_{loc,max}$ related to the full width at half maximum (FWHM), see also **Fig. 5**.

$$\text{Strain localization} = \frac{\varepsilon_{loc,max}}{FWHM} = \frac{\varepsilon_{v,max} - \varepsilon_w(F_{max})}{FWHM} \tag{3}$$

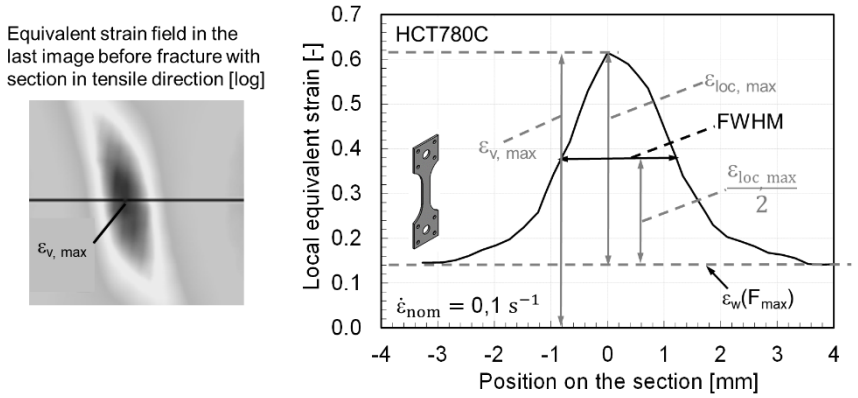

***Figure 5**: Definition of the relevant factors for the evaluation of the strain localization*

With increasing strain localization, the local equivalent strain rate increases for the investigated sheet steel materials, see **Fig. 6** on the left. With increasing hardening value $n_{2\text{-}Ag}$, the strain localization also increases at a comparable strain rate. This phenomenon, initially appearing counterintuitive, is elucidated by the observation that as the n value decreases, larger strain rates occur with consistent localization. **Fig. 6** on the right shows a linear correlation of the strain localization and the equivalent strain rate and can be approximately described by the following relationship (4). Here $\dot{\varepsilon}_v$ represents the local equivalent strain rate at the localization maximum.

$$\frac{\varepsilon_{loc,max}}{FWHM} \cong n_{2-A_g}\dot{\varepsilon}_v \tag{4}$$

Hence, under similar strain rate conditions, higher temperature gradients may arise with an increasing n-value, facilitating enhanced heat transfer from the localized zone to the

surrounding material. Also Frost and Ashby (1982) showed that the transition strain rate for the isothermal-adiabatic transition shifts towards higher strain rates with increasing n-value. Therefore materials with higher n-values undergo increased heat transfer at a comparable strain rate. Under shear loading, significant larger strain localizations occur than under tensile loading, see **Fig. 7**, as a reason for the increased heat transfer in shear bands compared to necking zones under tensile loading.

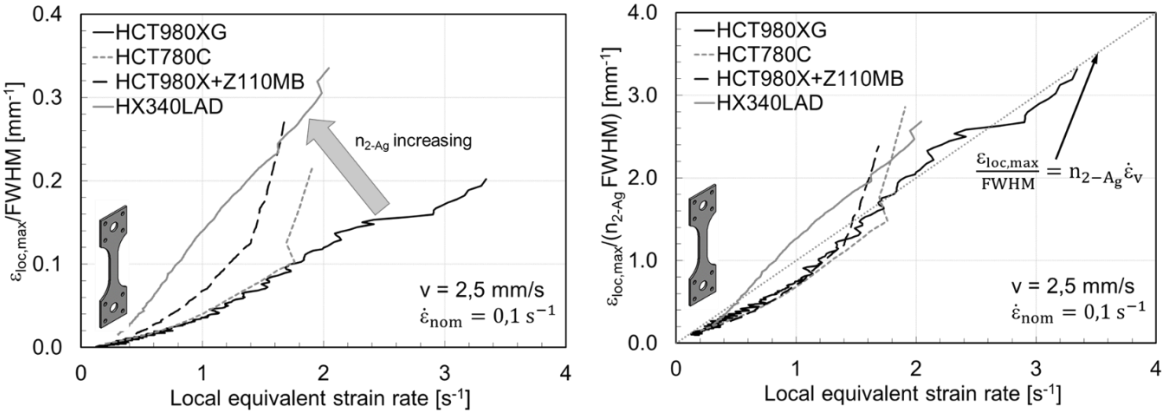

***Figure 6**: Strain localization (left) and n-value related strain localization (right) vs. local strain rate for tensile tests with a test speed of 2.5 mm/s for different AHSS*

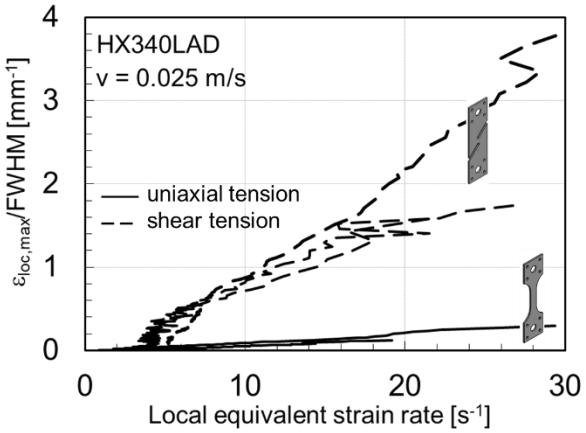

***Figure 7**: Strain localization dependent on the local strain rate for shear tests compared to tensile tests with a test speed of 0.025 mm/s for the micro-alloyed steel HX340LAD*

3 Conclusions

The aim was to investigate the factors influencing the isothermal-adiabatic transition region, particularly when shear bands occur. The results lead to the following conclusions:

- The isothermal-adiabatic transition region shows a dependency on the strain rate, the hardening behavior and the stress state. For a HCT980X steel under tensile loading the transition range is found between strain rates around 0.01 s^{-1} and 10 s^{-1}. For a HX340LAD with a larger n-value it is shifted to higher strain rates due to a slowdown of localization.

- The correlation between strain localization and equivalent strain rate can be estimated using a linear model, with the slope being determined by the n-value.
- Under shear loading the isothermal-adiabatic transition region occurs at higher strain rates compared to tensile loading. For the investigated AHSS approximately adiabatic conditions can be assumed at local strain rates from a magnitude of about 50 s^{-1}. This is attributed to substantially larger localizations at equivalent strain rates within the peak of shear localization, resulting in enhanced heat dissipation.

The findings are pertinent for determining the potential occurrence of adiabatic shear bands. This is applicable to the desired formation of adiabatic shear bands during adiabatic blanking processes, but can also be helpful in high-speed forming using electromagnetically accelerated tools or membrane pulse techniques. It is also relevant in the undesired occurrence of such bands to avert failure in safety-critical dynamically loaded structures. The results establish an empirical foundation for assessing the fraction of heat retained within the material within the isothermal-adiabatic transition region, considering the stress state (tensile or shear) and strain rate as well as material properties. This enables the estimation of localized temperature rises without complex thermomechanical coupling FE-simulations, even in scenarios involving heat dissipation, which is shown by Klitschke (2022).

References

Andrade, F., Conde, S., Feucht, M., Helbig, M. und Haufe, A., 2019, *Estimation of Stress Triaxiality from optically measured Strain Fields*, 12th European LS-DYNA Conference 2019, Koblenz, Germany.

Davidenkov, N., Mirolubov, I., 1935. Tech. Phys. USSR 2, pp. 281–298.

Dodd, B., Walley, S.M., Yang, R., Nesternko, V.F., 2015. *Major Steps in the Discovery of Adiabatic Shear Bands*. Metallurgical and Materials Transactions A. 46A.

Frost, H.J., Ashby, M.F., 1982. *Deformation-mechanism maps: the plasticity and creep of metals and ceramics*, Pergamon Press Oxford, pp. 120-123.

ISO 26203-2, 2011, *Metallic Materials – Tensile testing at high strain rates – Part 2: Servohydraulic and other test systems*, Beuth Verlag

Klitschke, S., 2022. Adiabatic heating of steel sheet materials under complex crash loads, University of Stuttgart, Institute for Metal Forming Technology, Germany

Kravz-Tarnavskii, V.P., 1928. J. Russ. Metall. Soc., issue 3, pp. 162-167.

Peirs, J., Verleysen, P., Degrieck, J., 2012. *Novel technique for static and dynamic shear testing of Ti6Al4V sheet*, Exp. Mech. 52 (7) pp. 729-741.

Richter, F., 2010. *Die physikalischen Eigenschaften der Stähle, Das "100-Stähle-Programm" Part I: Tables and Figures*, Forschungszentrum Karlsruhe.

Rittel, D., Zhang, L.H., Osovski, S., 2017. *The dependence of the Taylor-Quinney coefficient on the dynamic loading mode*, Journal of Mechanics and Physics of Solids 107, pp. 96-114

Taylor, G.I., Quinney, H., 1934. Proc. R. Soc. Lond. A. 143, pp. 307–326.

Walley, S.M., 2007. Metall. Mater. Trans. A 38A, pp. 2629–2654